

Spatio-temporal EEG activity in cortical network during visual perception task

Alexander Kuc

Neuroscience and Cognitive Technology Laboratory,
Center for Technologies in Robotics
and Mechatronics Components
Innopolis University,
Saratov, Russia.
kuc1995@mail.ru

Natalija Malova

Neuroscience and Cognitive Technology Laboratory,
Center for Technologies in Robotics
and Mechatronics Components
Innopolis University,
Innopolis, Russia.
malovanatalija@mail.ru

Abstract—A promising task is the analysis of the different rhythms of the brain cortical activity when performing cognitive tasks. Studying this issue allows to advance in the development of brain-computer interfaces. Some brain rhythms show certain dynamics during various cognitive activities. An important rhythm associated with cognitive activity is the alpha rhythm. In this paper, we study features of the dynamics of the alpha rhythm during bistable visual processing of information of varying complexity.

Index Terms—brain-computer interface, alpha-band activity, visual classification task, time-frequency analysis

I. INTRODUCTION

Studying the electrical activity of the brain is a very promising task that allows to advance in the development of brain-computer interfaces [1]. This activity consists of various neural rhythms, such as δ (1-5 Hz), θ (5-8 Hz), α (8-12 Hz), β (15-30 Hz) and γ (50-100 Hz). The activity of individual rhythms is manifested during various neurophysiological processes. Thus, alpha and beta rhythms play a significant role in processing visual information [2], [3]. Some studies also show that different rhythms and areas of the brain interact functionally when solving cognitive tasks [4]–[6].

Understanding the neurophysiological mechanisms of cognitive processes in the brain can significantly advance the development of passive neurointerfaces that monitor a person's cognitive state in real time [7].

In this paper, we study the dynamics of neural activity in the brain during a cognitive process such as visual perception of bistable images of varying complexity. For the study, we chose the alpha frequency range, as it is associated with processing visual information and changing the level of cognitive attention [8]–[10].

II. MATERIALS AND METHODS

A. Subjects

Ten healthy subjects (5 men and 5 women) aged 26 to 35 years with normal or corrected-to-normal visual acuity participated in the experiments. All of them gave informed written consent before participating in the experiment. The subjects were familiar with the experimental task, but did not participate in the experiments at least in the last 6 months before this experiment. The experimental studies were conducted in accordance with the Helsinki Declaration and approved by the local ethics Commission of Innopolis University.

B. Task

The Necker cube was used as the visual stimuli [11], [12]. It represents itself a cube with transparent faces and visible edges; an observer without any perception abnormalities sees the Necker cube as a 3D-object due to the specific position of the cube's edges. Bistability in perception consists in the interpretation of this 3D-object as to be either left- or right-oriented depending on the contrast of different inner edges of the cube. The contrast $a \in [0, 1]$ of the three middle lines centered in the left middle corner was used as a control parameter. The values $a = 1$ and $a = 0$ correspond, respectively, to 0 (black) and 255 (white) pixels luminance of the middle lines. Therefore, we can define a contrast parameter as $a = y/255$, where y is the brightness level of the middle lines using the 8-bit gray-scale palette. In our experiment we used Necker cube images with 8 different ambiguity levels (see Fig. 1). Half of them, $a \in \{0.15, 0.25, 0.4, 0.45\}$ were left-oriented, while another half, $a \in \{0.55, 0.6, 0.75, 0.85\}$ were right-oriented. While for $a = 0$ and $a = 1$ the Necker cubes orientation can easily be interpreted as a left or a right, for $a \sim 0.5$ the identification of the actual orientation becomes more complex since we deal with a highly ambiguous image.

Each Necker cube image drawn by black and gray lines was located at the center of the computer screen on a white

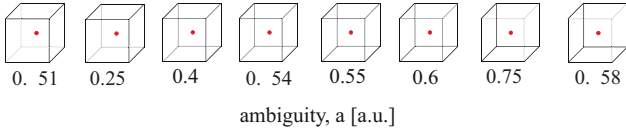


Fig. 1. The set of visual stimuli (Necker cubes) with the different degree of ambiguity a

background. A red dot drawn at the center of the Necker cube was used to attract subject's attention and prevent possible perception shifts due to eye movements while observing the image. The stimuli were demonstrated on a 24" BenQ LCD monitor with a spatial resolution of 1920×1080 pixels and a 60 Hz refresh rate. The subjects were located at a distance of 70–80 cm from the monitor with a visual angle of approximately 0.25 rad. The Necker cube size on the monitor was 14.2 cm.

C. Experimental protocol

The whole experiment lasted about 40 min for each participant, including short EEG recordings at rest (~ 4 min) before and after the main part of the experiment. During experimental sessions, cubes with predefined values a (from the set illustrated in Fig. 1) were randomly represented 400 times (each cube with a certain ambiguity was represented about 50 times) [13].

Participants were asked to press either the left or right key to indicate the first impression of the orientation of each cube. Since the sequential presentation of images previously demonstrated cubes can affect the perception of subsequent, the duration of the demonstration of the stimulus varied in the range of 1–1.5 seconds. In addition, a random change in parameter a also prevented the stabilization of perception. Finally, to distract the observer's attention and make the perception of the next Necker cube independent of the previous one, abstract images were shown for 3–5 seconds between subsequent demonstrations of the cube images [12].

D. Recording

To register the EEG data, the cup adhesive Ag/AgCl electrodes were placed on the scalp using the classical extended ten–ten electrode system. The electrodes were installed with "Tien–20" paste (Weaver and Company, Colorado, USA). Electrical activity was recorded using 31 electrodes. Before the experiment, we put the abrasive "NuPre" gel on the scalp to increase its conductivity. After the electrodes were installed, we monitored the impedance during the experiments, which varied in the interval of 2–5 k Ω . The ground electrode N was located above the forehead, and reference electrodes A_1 and A_2 were attached to the mastoids. For filtering the EEG signals, we used a band-pass filter with cut-off points at 0.016 Hz (HP) and 70 Hz (LP), as well as a 50-Hz Notch filter. For EEG and EOG signal amplification and analog-to-digital conversion; the electroencephalograph "Encephalan–EEGR–19/26" ("Medikom-MTD", Taganrog, Russia).

E. EEG analysis

We analyzed the EEG signals power in α -frequency band (8–12 Hz), using the continuous wavelet transformation. The wavelet power spectrum $E^n(f, t) = (W^n(f, t))^2$ was calculated for each EEG channel $X_n(t)$ in the frequency range $f \in [1, 30]$ Hz. Here, $W^n(f, t)$ is the complex-valued wavelet coefficients calculated as

$$W^n(f, t) = \sqrt{f} \int_{t-4/f}^{t+4/f} X_n(t) \psi^*(f, t) dt, \quad (1)$$

where $n = 1, \dots, N$ is the EEG channel number ($N = 31$ is the total number of channels used for the analysis) and "*" defines the complex conjugation. The mother wavelet function $\psi(f, t)$ is the Morlet wavelet [14] which is defined as

$$\psi(f, t) = \sqrt{f} \pi^{1/4} e^{j\omega_0 f(t-t_0)} e^{f(t-t_0)^2/2}, \quad (2)$$

where $\omega_0 = 2\pi$ is the wavelet parameter.

Then, for α -frequency band the wavelet amplitude $E_\alpha^n(t)$ were calculated as

$$E_\alpha^n(t) = \frac{1}{\Delta f_\alpha} \int_{\Delta f_\alpha} E^n(f', t) df', \quad (3)$$

where $\Delta f_\alpha = 8–12$ Hz. The time-series of the wavelet power (3) was calculated for the whole time of the experimental session and then was split into the time segments $\tau_{\text{pre}}^i = 0.5$ s and $\tau_{\text{post}}^i = 0.5$ s, before and after the i -th visual stimulus presentation.

$$\langle E_\alpha^n \rangle_{\tau_{\text{pre}}^i, \tau_{\text{post}}^i} = \int_{\tau_{\text{pre}}^i, \tau_{\text{post}}^i} E_\alpha^n(t') dt'. \quad (4)$$

For each stimulus ambiguity the difference between $\langle E_{\alpha, \beta}^n \rangle_{\tau_{\text{pre}}^i}$ and $\langle E_{\alpha, \beta}^n \rangle_{\tau_{\text{post}}^i}$ for the n -th EEG sensor was analyzed statistically via the paired samples t-test based on 20 trials.

III. RESULTS

To investigate the effect of visual stimulus complexity, all Necker cubes were divided into two groups (Fig. 2):

- Low ambiguity (LA) stimuli, including the Necker cube images with $a \in \{0.15, 0.25, 0.75, 0.85\}$
- High ambiguity (HA) stimuli, including the Necker cube images with $a \in \{0.4, 0.45, 0.55, 0.6\}$

Each group included 80 stimuli (20 per each ambiguity). EEG features were analyzed and compared for LA and HA stimuli for two moments of time: $t_1 = 0.25$ s and $t_2 = 0.5$ s after the image presentation. Fig. 3 and Fig. 4 demonstrates difference D between the number of EEG channels, where E_α increases and those where E_α decreases for LA and HA trials at both time moments. These diagrams show the distribution of these values in the participant groups (median, 25th and 75th percentiles).

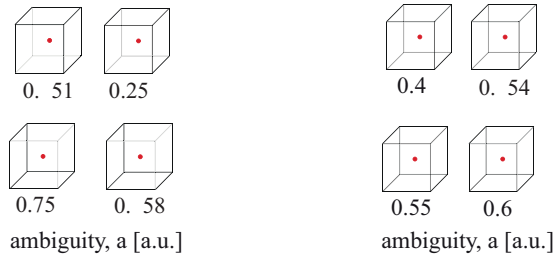


Fig. 2. Visual stimuli divided into two groups according to their ambiguity

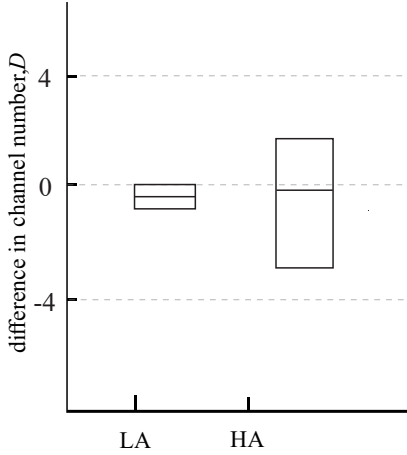


Fig. 3. The difference D between the number of channels where the EEG amplitude in the alpha range (E_α) increases and the number of channels where E_α decreases depending on the ambiguity of the stimuli (LA, HA) for t_1 time moment

Figure 3 shows that at t_1 time for both groups of stimuli, the proportion of channels with decreasing and increasing α -rhythm energy is the same (median $D \sim 0$).

However, at the t_2 time the predominance of EEG channels with decreasing energy in the α -frequency range is recorded (median $D = -1.75$ and $D = -2.5$ for LA and HA stimuli respectively) (Fig. 4).

Then, to compare the differences D between all the conditions, we used repeated measures ANOVA. Image ambiguity levels (HA and LA) and time points (t_1 , t_2) were used as within-subject factors. ANOVA with Greenhouse-Geisser correction reveals significant difference of D between time moments ($F_{1,9} = 8.28, p = 0.018$) while the difference between HA and LA stimuli is insignificant ($F_{1,9} = 0.25, p = 0.877$). Wilcoxon signed rank test for the related samples did not revealed significant change between LA and HA groups.

Therefore, after the visual stimulus is presented at time t_2 , the number of EEG channels showing a decrease in activity in the α -range increases relative to time t_1 . From this we can conclude that the processing of visual information is associated with a decrease in the activity of the α -rhythm.

We have constructed a topographical graph showing a decrease in α -frequency band activity for the LA (b) and HA

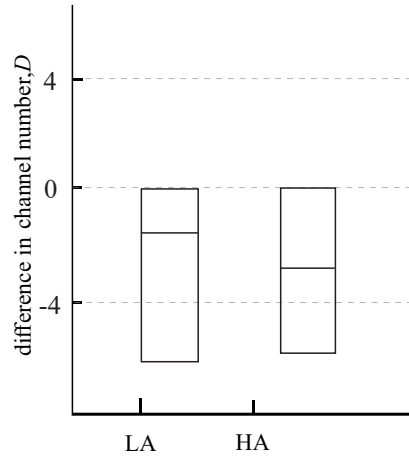


Fig. 4. The difference D between the number of channels where the EEG amplitude in the alpha range (E_α) increases and the number of channels where E_α decreases depending on the ambiguity of the stimuli (LA, HA) for t_2 time moment

(c) trials for the t_2 time point (Fig. 5). A higher amplitude means that more subjects show a decrease in energy in a given area of the brain. The graph shows that the majority of subjects have decreased activity in the alpha range in the parietal region (P3, Pz, P4).

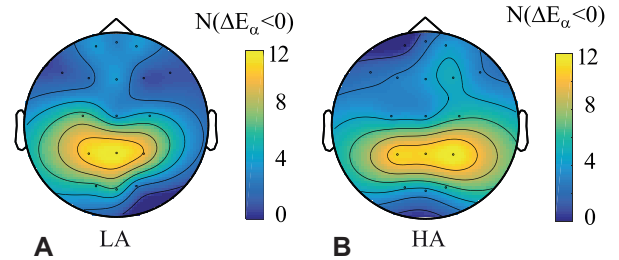


Fig. 5. Topographical plot of the distribution of EEG channels reflecting E_α decrease for all subjects for LA (a) and HA (b) stimuli

IV. CONCLUSION

In this paper we have considered the cortical activity in the alpha-frequency band during the visual information processing. It is shown that during the processing of both simple and complex visual information, the alpha-band power decreases in the parietal zone. Although our results do not demonstrate the difference between the alpha-band activity for the different complexity, they can be utilized as the biomarker of the cognitive load. Thus, the results of this study can be useful in the development of passive neurointerfaces that monitor the cognitive state of a person during the visual task accomplishment.

ACKNOWLEDGMENT

This study is supported by the President Program (MK-1760.2020.2) in the part of experimental analysis. Data analysis is supported by the President Program (NSH-2594.2020.2).

REFERENCES

- [1] V. A. Maksimenko, A. E. Hramov, N. S. Frolov, A. Lüttjohann, V. O. Nedaivozov, V. V. Grubov, A. E. Runnova, V. V. Makarov, J. Kurths, and A. N. Pisarchik, "Increasing human performance by sharing cognitive load using brain-to-brain interface," *Frontiers in neuroscience*, vol. 12, p. 949, 2018.
- [2] V. A. Maksimenko, A. E. Runnova, N. S. Frolov, V. V. Makarov, V. Nedaivozov, A. A. Koronovskii, A. Pisarchik, and A. E. Hramov, "Multiscale neural connectivity during human sensory processing in the brain," *Physical Review E*, vol. 97, no. 5, p. 052405, 2018.
- [3] G. Michalareas, J. Vezoli, S. Van Pelt, J.-M. Schoffelen, H. Kennedy, and P. Fries, "Alpha-beta and gamma rhythms subserve feedback and feedforward influences among human visual cortical areas," *Neuron*, vol. 89, no. 2, pp. 384–397, 2016.
- [4] R. T. Canolty, E. Edwards, S. S. Dalal, M. Soltani, S. S. Nagarajan, H. E. Kirsch, M. S. Berger, N. M. Barbaro, and R. T. Knight, "High gamma power is phase-locked to theta oscillations in human neocortex," *science*, vol. 313, no. 5793, pp. 1626–1628, 2006.
- [5] J. E. Lisman and O. Jensen, "The theta-gamma neural code," *Neuron*, vol. 77, no. 6, pp. 1002–1016, 2013.
- [6] P. Fries, "Rhythms for cognition: communication through coherence," *Neuron*, vol. 88, no. 1, pp. 220–235, 2015.
- [7] V. A. Maksimenko, A. E. Hramov, V. V. Grubov, V. O. Nedaivozov, V. V. Makarov, and A. N. Pisarchik, "Nonlinear effect of biological feedback on brain attentional state," *Nonlinear Dynamics*, vol. 95, no. 3, pp. 1923–1939, 2019.
- [8] P. Sauseng, W. Klimesch, W. Stadler, M. Schabus, M. Doppelmayr, S. Hanslmayr, W. R. Gruber, and N. Birbaumer, "A shift of visual spatial attention is selectively associated with human eeg alpha activity," *European Journal of Neuroscience*, vol. 22, no. 11, pp. 2917–2926, 2005.
- [9] J. J. Foxe and A. C. Snyder, "The role of alpha-band brain oscillations as a sensory suppression mechanism during selective attention," *Frontiers in psychology*, vol. 2, p. 154, 2011.
- [10] V. A. Maksimenko, A. E. Runnova, M. O. Zhuravlev, V. V. Makarov, V. Nedayvozov, V. V. Grubov, S. V. Pchelintceva, A. E. Hramov, and A. N. Pisarchik, "Visual perception affected by motivation and alertness controlled by a noninvasive brain-computer interface," *PloS one*, vol. 12, no. 12, 2017.
- [11] J. Kornmeier, E. Friedel, M. Wittmann, and H. Atmanspacher, "Eeg correlates of cognitive time scales in the necker-zeno model for bistable perception," *Consciousness and cognition*, vol. 53, pp. 136–150, 2017.
- [12] A. E. Hramov, V. A. Maksimenko, S. V. Pchelintseva, A. E. Runnova, V. V. Grubov, V. Y. Musatov, M. O. Zhuravlev, A. A. Koronovskii, and A. N. Pisarchik, "Classifying the perceptual interpretations of a bistable image using eeg and artificial neural networks," *Frontiers in neuroscience*, vol. 11, p. 674, 2017.
- [13] V. A. Maksimenko, N. S. Frolov, A. E. Hramov, A. E. RUNNOVA, V. V. Grubov, J. Kurths, and A. N. Pisarchik, "Neural interactions in a spatially-distributed cortical network during perceptual decision-making," *Frontiers in behavioral neuroscience*, vol. 13, p. 220, 2019.
- [14] A. E. Hramov, A. A. Koronovskii, V. A. Makarov, A. N. Pavlov, and E. Sitnikova, *Wavelets in neuroscience*. Springer, 2015.